Supporting Information

Ptacin et al. 10.1073/pnas.1405188111

Construction of Plasmids

General. PCR was carried out using KOD hotstart DNA polymerase (Novagen). Restriction digestion was performed using Fermentas Fast Digest or New England Biolabs enzymes, and ligations were performed using Fermentas Rapid Ligation buffer and ligase. All plasmid constructs were sequence-verified for correct insert sequence. Quickchange mutagenesis was performed using Pfu Ultra polymerase (Stratagene).

Details of Individual Plasmid Construction. The plasmid pJP232 was generated by digesting the plasmid pJP45 (1) with NdeI and SacI and ligating the resulting *parA* G16V coding sequence into the NdeI/SacI sites in the plasmid pVYFPC-5 (2).

The plasmid pJP264 was generated by PCR amplification of the *tipN-mcherry* coding sequence from the plasmid pGB404 [tipN-mcherry coding sequence in the NdeI/AgeI sites of the plasmid pRVMCS-5 (2)] using PCR primers that added NdeI and XbaI restriction sites to the 5′ and 3′ ends, respectively. This product was then inserted into the NdeI/XbaI sites in the plasmid pBXMCS-4 (2).

The plasmid pJP62 was generated by PCR amplification of the *Caulobacter crescentus parA* gene using the primers GATCAGACTAGTCCGCTAATCCTCTCCGCGTTCTGGCT and GACTTCTAGATTACTTGTCGTCGTCGTCCTTGTAGTCGGCGGCCTTGGCCTGGCGATCGCGTTC, which add a 5′ SpeI restriction site and a 3′ Flag epitope, stop codon, and XbaI restriction site. Another PCR amplified the genomic region 3′ of the *parA* gene using the primers GTACAGtctagaGTCCAAAGAACAAGAACCGTAGCTTGACTGAG and GATCAGACTAGTTCAGATCCCGCGCGTCAGTCG, which added XbaI and SpeI sites to the 5′ and 3′ ends, respectively. These products were ligated simultaneously into the SpeI site of the plasmid pNPTS138 (M. R. Alley, method described in ref. 3).

The plasmid pJP325 was generated by PCR amplification of the *parA* gene adding NcoI and SacI restriction sites to the 5′ and 3′ ends, respectively. This product was inserted into the NcoI and SacI sites of the plasmid pET28b.

The plasmid pJP137 was generated by PCR amplification of the *parB* gene, adding NdeI and a stop codon/BamHI restriction site to the 5′ and 3′ ends, respectively. This product was inserted into the NdeI/BamHI sites in the plasmid pET28b.

The plasmid pJP382 was generated by colony PCR amplification of the *popZ-S22P* gene from the plasmid pJP318, which contains the *popZ-S22P* gene in the NcoI/EcoRI sites in the plasmid pBad/HisA, adding 5′ NdeI and 3′ stop codon/SacI restriction sites. This product was inserted into the NdeI and SacI sites of the plasmid pET28b.

The plasmid pJP383 was generated by Quickchange mutagenesis of the plasmid pGB165 (4).

The plasmid pJP408 was generated by Quickchange mutagenesis of the plasmid pJP383 using the primers GTCATCCTCCGGGATGATTTCTCGAATGGAGGCGAG and CTCGCCTCCATTCGAGAAATCATCCCGGAGGATGAC.

The plasmid pGB759 was generated by PCR amplification of the *mcherry-popZ* gene from the plasmid pJP242 [*popZ* gene with a stop codon inserted into the KpnI and EcoRI sites of the plasmid pXCHYN-2 (2)], adding 5′ XbaI and 3′ stop codon/ EcoRI restriction sites. This product was inserted into the XbaI and EcoRI sites in the plasmid pASK-IBA3+.

The plasmid pJP410 was generated by PCR amplification of the *mcherry-popZ-KE* gene from the plasmid pJP322 (*popZ-KE* gene in the KpnI/EcoRI sites in the plasmid pXCHYN-2) adding 5′ XbaI and 3′ stop codon/ EcoRI restriction sites. This product was inserted into the XbaI and EcoRI sites in the plasmid pASK-IBA3+.

The plasmid pJP411 was generated by PCR amplification of the *mcherry-popZ-SP* gene, and adding 5′ XbaI and 3′ stop codon/ EcoRI restriction sites. This product was inserted into the XbaI and EcoRI sites in the plasmid pASK-IBA3+.

The plasmid pJP186 was generated by PCR amplification of the *parB* gene, adding 5′ NcoI and 3′ stop codon/ NotI restriction sites. This product was inserted into the NcoI and NotI sites in the plasmid pCDFduet1.

Plasmid 118 was generated by PCR amplification of the *parA-G16V* gene from the plasmid pJP94, adding 5′ NdeI and 3′ AvrII restriction sites. This product was inserted into the NdeI and AvrII sites in the plasmid pJP10 [pACYCduet1-*cfp-parB* (1)].

The plasmid pJP414 was generated by PCR amplification of the *popZ* gene adding 5′ NcoI and 3′ stop codon/ EcoRI restriction sites. This product was inserted into the NcoI and EcoRI sites in the plasmid pBad/HisA.

The plasmid pJP415 was generated by PCR amplification of the *popZ-KE* gene adding 5′ NcoI and 3′ stop codon/ EcoRI restriction sites. This product was inserted into the NcoI and EcoRI sites in the plasmid pBad/HisA.

The plasmid pJP417 was generated by PCR amplification of the *popZ-KEP* gene adding 5′ NcoI and 3′ stop codon/ EcoRI restriction sites. This product was inserted into the NcoI and EcoRI sites in the plasmid pBad/HisA.

The plasmid pJP318 was generated by PCR amplification of the *popZ-SP* gene adding 5′ NcoI and 3′ stop codon/ EcoRI restriction sites. This product was inserted into the NcoI and EcoRI sites in the plasmid pBad/HisA.

The plasmid pJP289 was generated by PCR amplifying the genomic region 5′ of the *popZ* gene with the primers aaattaagcttGACGGTCTCGGCGCGCGCTT and aaaacatatgGTGCGGGGCCGTCGTAAAGA, which add a HindIII and NdeI site to the 5′ and 3′ ends, respectively. The *mcherry-popZ* coding sequence was amplified from the plasmid pJP242 (5) with the primers TTCATatggtgagcaagggcgagga and tttttggtaccCTTGTACAGCTCGTCCATG, which add a 5′ NdeI and a 3′ stop codon and EcoRI restriction site. These products were simultaneously inserted into the NdeI and EcoRI sites in the plasmid pMCS-4.

To construct the plasmid pJP387, the *popZ-KE* gene was PCR amplified from the plasmid pJP322, adding a 5′ KpnI and 3′ stop codon and EcoRI restriction site. This product was inserted into the KpnI and EcoRI sites in the plasmid pJP289.

To construct the plasmid pJP312, the *popZ-SP* gene was PCR amplified, adding a 5′ KpnI and 3′ stop codon and EcoRI restriction site. This product was inserted into the KpnI and EcoRI sites in the plasmid pJP289.

To construct the plasmid pJP347, the *popZ-KEP* gene was PCR amplified from the plasmid pGB964 [contains the *popZ-KEP* gene in the NdeI and EcoRI sites of the plasmid pBXMCS-4 (2)], adding a 5′ KpnI and 3′ stop codon and EcoRI restriction site. This product was inserted into the KpnI and EcoRI sites in the plasmid pJP289.

To construct the plasmid pJP403, the *popZ* gene was PCR amplified, adding 5′ KpnI and 3′ stop codon and EcoRI restriction sites. This product was inserted into the KpnI and EcoRI sites in the plasmid pXYFPN-4 (2).

To construct the plasmid pJP413, the *pamCherry* coding sequence was PCR amplified from the plasmid pAmCherry-N1 (Clontech), adding a 5′ NdeI and 3′ KpnI restriction site. This

product was inserted into the NdeI and KpnI sites of the plasmid pJP242 (5). Next, the *pamcherry-popZ* gene was released from this plasmid using NdeI and EcoRI and inserted into these sites in the plasmid pVCHYN-5 (2).

To construct the plasmid pJP420, the *parA-GV* gene was released from the plasmid pJP45 [pXYFPC5-*parA* G16V (1)] using NdeI and SacI, and inserted into these sites in the plasmid pXYFPC-2 (2).

To construct plasmid 248, the *popZ-SP* gene was PCR amplified adding 5′ NdeI and 3′ stop codon and EcoRI restriction sites. This product was inserted into the NdeI and EcoRI sites in the plasmid pBXMCS-4 (2).

To construct the plasmid pGB908, the *popZ-KE* gene was PCR amplified adding 5′ NdeI and 3′ stop codon and EcoRI restriction sites. This product was inserted into the NdeI and EcoRI sites in the plasmid pBXMCS-4 (2).

To construct the plasmid pJP384, the *parB* gene was PCR amplified adding a 5′ KpnI and 3′ stop codon and NheI restriction site. This product was inserted into the KpnI and NheI sites in the plasmid pXYFPN-2 (2).

1. Ptacin JL, et al. (2010) A spindle-like apparatus guides bacterial chromosome segregation. *Nat Cell Biol* 12(8):791–798.
2. Thanbichler M, Iniesta AA, Shapiro L (2007) A comprehensive set of plasmids for vanillate- and xylose-inducible gene expression in Caulobacter crescentus. *Nucleic Acids Res* 35(20):e137.
3. Thanbichler M, Shapiro L (2006) MipZ, a spatial regulator coordinating chromosome segregation with cell division in Caulobacter. *Cell* 126(1):147–162.
4. Bowman GR, et al. (2008) A polymeric protein anchors the chromosomal origin/ParB complex at a bacterial cell pole. *Cell* 134(6):945–955.
5. Bowman GR, et al. (2010) Caulobacter PopZ forms a polar subdomain dictating sequential changes in pole composition and function. *Mol Microbiol* 76(1):173–189.

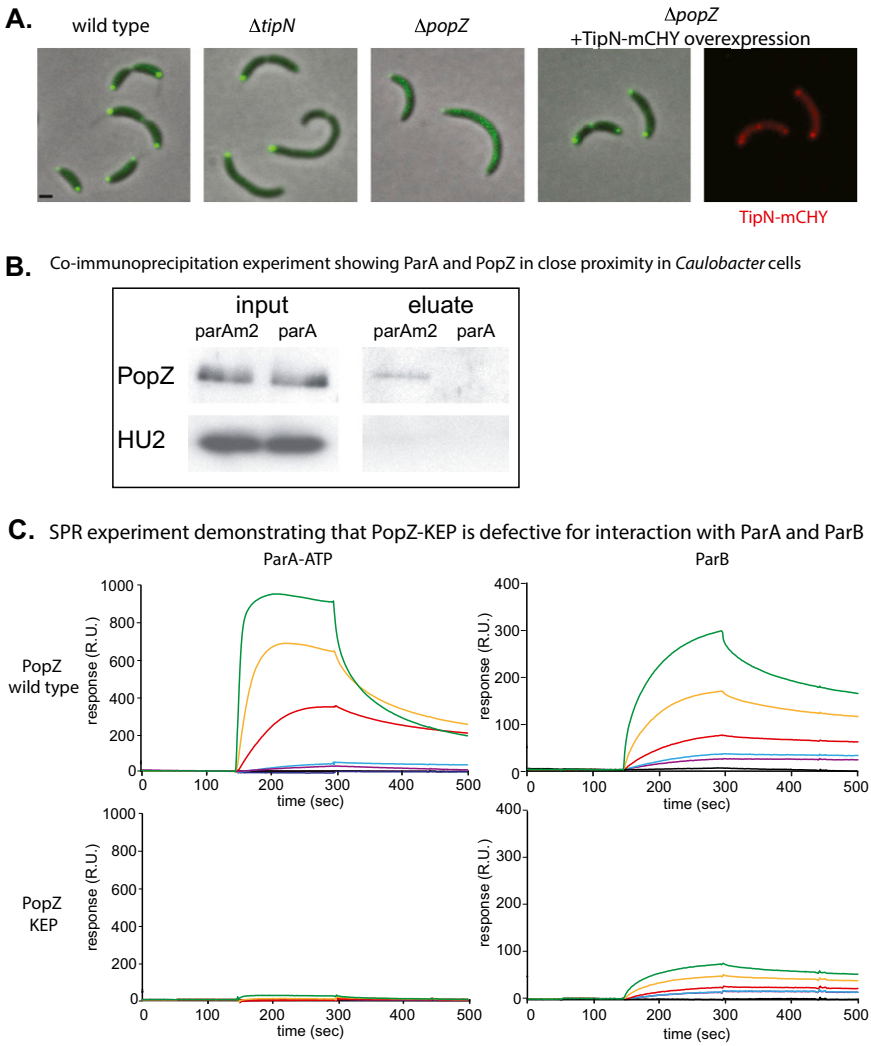

Fig. S1. Data supporting a direct interaction between ParA and PopZ in vitro and in vivo. (*A*) PopZ is required for ParA recruitment to the *Caulobacter* cell pole, but TipN overexpression can rescue ParA recruitment in Δ*popZ* cells. Images of *Caulobacter* cells expressing $ParA_{G16V}$ -eYFP protein (a monomeric form of ParA that is recruited to the cell pole) in the indicated genetic backgrounds are shown with phase-contrast and eYFP (green) or mCherry (red) fluorescence overlaid. (Scale bar, 1μm.) (*B*) Coimmunoprecipitation assay showing that ParA forms a complex with PopZ in *Caulobacter*. Samples of whole cell lysates (input) from strain JP88 (parA-m2) and wild-type cells (parA) and immunoprecipitated protein complexes (eluate) were probed with anti-PopZ or anti-HU2 (an abundant nonspecific DNA binding protein) by Western blot. An anti-PopZ reactive band running at the predicted molecular weight of PopZ is observed specifically in the parA-m2 eluate, and no HU2 band was observed in eluate fractions, indicating that the observed ParA-PopZ interaction is unlikely to be nonspecific or indirect through another DNA binding protein (such as ParB, which interacts with both partners). (*C*) PopZ-KEP is defective in interaction with both ParA and ParB. Surface plasmon resonance experiments using immobilized 6His-PopZ (*Upper*) or 6His-PopZ-KEP (*Lower*). ParA-ATP (*Left*) or ParB (*Right*) was injected at the indicated concentrations at t = 150 s, followed by buffer only at t = 300 s. Response units (R.U.s) are plotted versus time (seconds).

A. Growth curves of *popZ* mutant strains cultured in PYE (rich media)

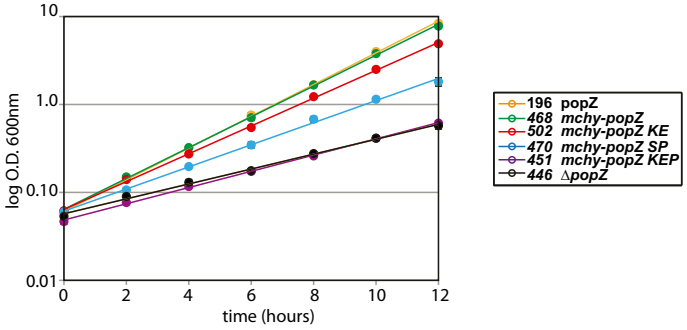

B. Growth curves of *popZ* mutant strains cultured in M2G (minimal media with glucose)

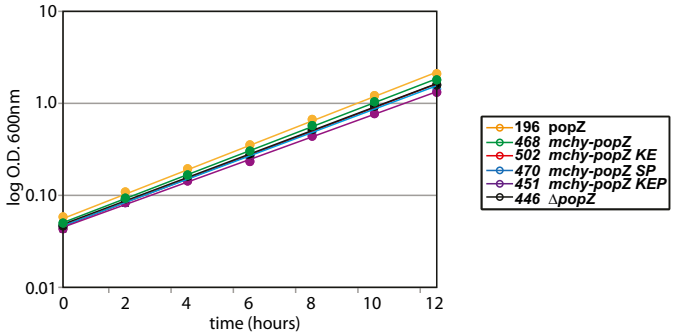

C. Table of growth and cell length characteristics of *popZ* mutant strains in PYE and M2G

Strain	PYE medium	M2G medium	
	generation (min) (mean+/- SEM)	cell length (um) (mean+/- STDEV)	generation (min) (mean+/- SEM)
JP196 wild type	106.7 +- 0.2	2.81 +- 0.72	139.6 +- 8
JP468 *mcherry-popZ*	109.4 +- 2.6	2.76 +- 0.70	143.8 +- 7
JP502 *mcherry-popZ KE*	119.2 +- 2.4	3.10 +- 1.21	145.1 +- 15
JP470 *mcherry-popZ SP*	159.5 +- 1.9	4.98 +- 2.31	157.3 +- 22
JP451 *mcherry-popZ KEP*	198.1 +- 1.3	5.29 +- 2.42	149.6 +- 8
JP446 ΔpopZ	222.1 +- 7.8	5.05 +- 2.30	147.2 +- 17

* doubling times measured as exponential curve fits to means of three independent replicates (all r2 > .97) expressed as mean and SEM

Fig. S2. *popZ* alleles that cause defective ParA and/or ParB interactions with PopZ disrupt growth and cell division in *Caulobacter*. (*A*) Mutant *popZ* alleles cause cell growth defects compared with wild-type *Caulobacter* cells when grown in rich media. Growth curves of mutant *popZ* strains cultured in peptone-yeast extract (PYE) media. Log scale plot of cell density (Abs_{600nm}) over time in hours (plots represent the mean of three independent replicates). Growth defects observed in mutant *popZ* alleles cultured in PYE are coincident with cell division defects and cell length variability (not shown). (*B*) Mutant *popZ* alleles cause only minor cell growth rate defects compared with wild-type *Caulobacter* cells when grown in minimal media. Growth curves of mutant *popZ* strains cultured in M2G media. Log scale plot of cell density (Abs_{600nm}) plotted over time in hours (plots represent the mean of three independent replicates). Despite similar doubling times in M2G, mutant *popZ* strains cultured in M2G demonstrate severe cell division defects and cell length variability (Fig. 3 *A* and *B*). (*C*) Table of growth and cell length characteristics of *popZ* mutant strains cultured in PYE and M2G.

A. Quantitation of PopZ signal localized to the cell pole in *popZ* mutant strains

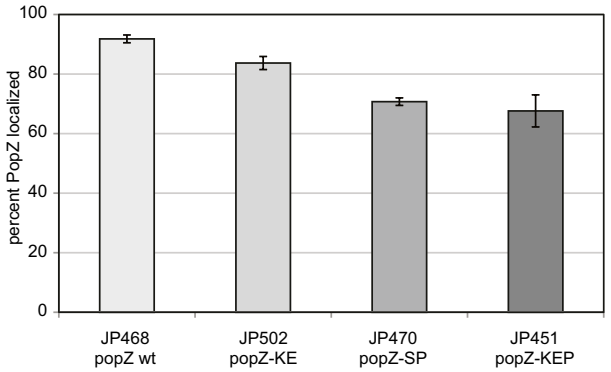

B. Quantitation of PopZ foci localization in *popZ* mutant strains

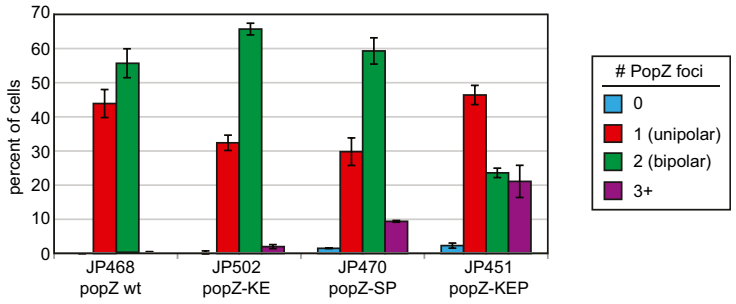

Fig. S3. *popZ* mutant alleles do not significantly affect PopZ assembly or localization in vivo. (*A*) mCherry-PopZ variants are not defective in focus formation in *Caulobacter*. The percent of mCherry-PopZ signal localized to the cell poles is shown for the indicated strains. Error bars indicate SEM of three independent replicates of $n > 30$ cells per experiment. The ~20% increase in delocalized mCherry-PopZ in the mutant strains cannot account for the significant cell morphology and cell division defects; recent work demonstrates that as much as 40% of PopZ may be delocalized without significant alterations to cell morphology and division (1, 2). (*B*) mCherry-PopZ variants are not defective in bipolar foci formation in *Caulobacter*. The frequency of mCherry-PopZ foci numbers per cell were quantitated (*Materials and Methods*), and the percent of cells with zero or one (unipolar), two (bipolar), or three or more mCherry-PopZ foci is plotted for the indicated strains. Error bars indicate SEM of three independent replicates of $n > 300$ cells. The results indicate that the *mcherry-popZ* alleles studied are not significantly defective in normal polar distribution in vivo.

1. Bowman GR, et al. (2013) Oligomerization and higher-order assembly contribute to sub-cellular localization of a bacterial scaffold. *Mol Microbiol* 90(4):776–795.
2. Laloux G, Jacobs-Wagner C (2013) Spatiotemporal control of PopZ localization through cell cycle-coupled multimerization. *J Cell Biol* 201(6):827–841.

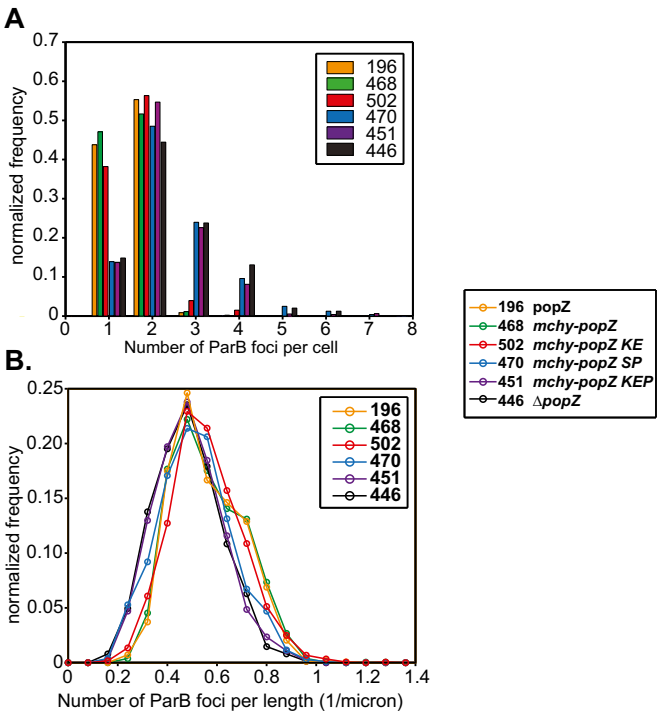

C Table of ParB foci number statistics from *popZ* mutant strains shown above

Strain	ParB foci per cell (mean+/- SD) n >638 cells	ParB foci per um (mean+/- SD) n >638 cells
JP196 wild type	1.57 +/- 0.51	0.56 +/- 0.15
JP468 *mcherry-popZ*	1.54 +/- 0.53	0.56 +/- 0.14
JP502 *mcherry-popZ KE*	1.69 +/- 0.64	0.56 +/- 0.15
JP470 *mcherry-popZ S22P*	2.44+/- 1.06	0.51+/- 0.15
JP451 *mcherry-popZ KEP*	2.49 +/-1.10	0.49 +/-0.14
JP446 Δ*popZ*	2.29 +/-0.86	0.48 +/-0.14

Fig. S4. Mutant *popZ* alleles do not affect ParB focus duplication or separation in *Caulobacter*. (*A*) Mutant *popZ* strains contain increased numbers of ParB foci per cell compared with wild type. The numbers of ParB foci per cell were computationally quantitated (*Materials and Methods*) for the indicated strains cultured in M2G media, and the normalized frequency of ParB foci number per cell is plotted. (*B*) Mutant *popZ* strains display comparable numbers of ParB foci per unit cell length. The normalized frequency of ParB foci number per micrometer of cell length is plotted for the indicated strains. The distributions of all strains are similar with mean 0.53 ± 0.14 foci (SD) per cell, indicating that mutant *popZ* strains are not grossly defective in DNA replication or ParB focus duplication/separation. (*C*) Table of ParB foci number statistics from *popZ* mutant strain data shown in *A* and *B*.

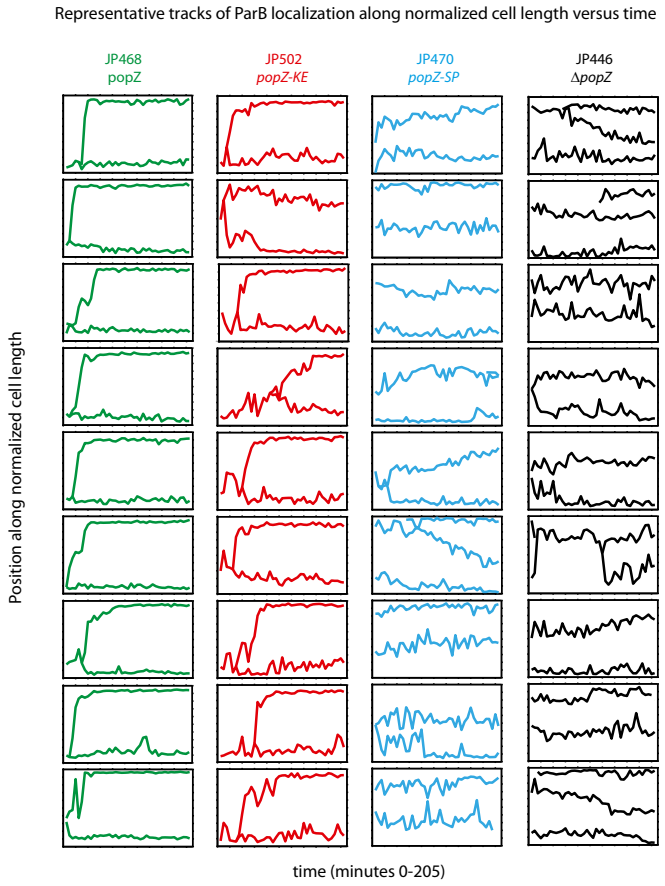

Fig. S5. Mutant *popZ* alleles cause severe ParB segregation defects characterized by erratic reverse segregation events. Mutant *popZ* alleles that prevent PopZ/ParA interactions cause erratic ParB segregation dynamics in *Caulobacter*. Strains were synchronized and the positions of CFP-ParB foci along normalized cell length are plotted versus time (imaging interval 5 min). Shown are several representative tracks of ParB foci position from JP468 (*popZ-wt*, green), JP502 (*popZ-KE*, red), JP470 (*popZ-SP*, blue), and JP446 (Δ*popZ*, black) strains.

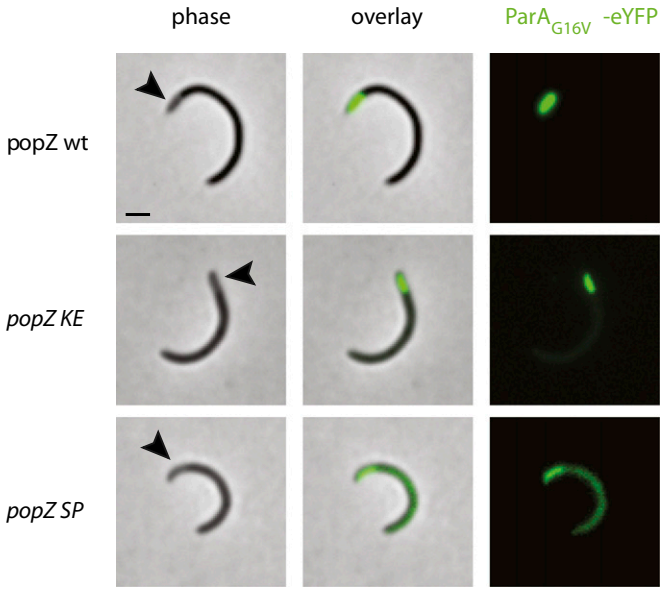

Fig. S6. Overexpressed PopZ forms large structures at the *Caulobacter* cell pole that recruit ParA throughout the PopZ matrix. PopZ "plug" colocalization assay in which untagged PopZ (or indicated mutant) is overexpressed in *Caulobacter* Δ*popZ* to form extended complexes at the cell pole (black arrow indicating polar phase-bright regions (1–3) that recruit ParA$_{G16V}$-eYFP (green). Fluorescence images are overlaid as shown. (Scale bar, 1 μm.)

1. Bowman GR, et al. (2008) A polymeric protein anchors the chromosomal origin/ParB complex at a bacterial cell pole. *Cell* 134(6):945–955.
2. Ebersbach G, Briegel A, Jensen GJ, Jacobs-Wagner C (2008) A self-associating protein critical for chromosome attachment, division, and polar organization in caulobacter. *Cell* 134(6): 956–968.
3. Laloux G, Jacobs-Wagner C (2013) Spatiotemporal control of PopZ localization through cell cycle-coupled multimerization. *J Cell Biol* 201(6):827–841.

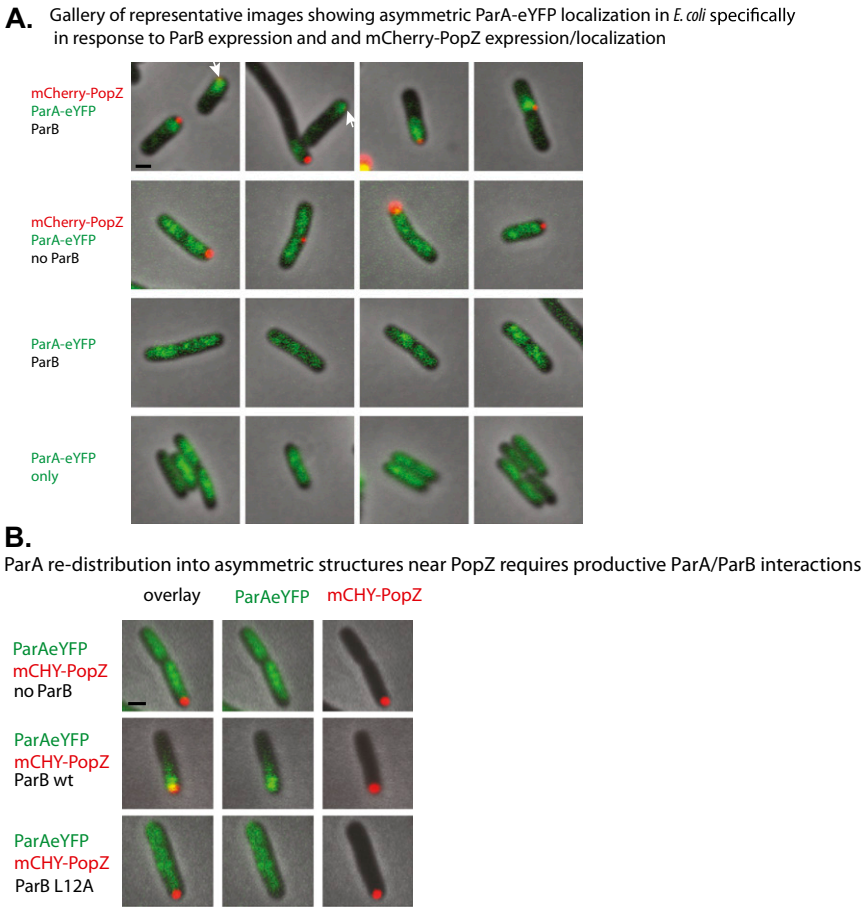

Fig. S7. ParB stimulates ParA localization into asymmetric structures near PopZ foci in *Escherichia coli*. (*A*) Gallery of representative images of *E. coli* cells expressing wild-type ParA-eYFP (green) in the presence or absence of mCherry-PopZ (red) and ParB (untagged) expression. White arrowheads indicate dim mCherry-PopZ foci that cause large-scale ParA relocalization. (Scale bar, 1 μm.) (*B*) ParA redistribution into asymmetric structures near PopZ requires productive ParA/ParB interactions. Images of *E. coli* cells expressing wild-type ParA-eYFP (green) and mCherry-PopZ (red) in the presence or absence of ParB or $ParB_{L12A}$ expression. (Scale bar, 1 μm.)

Table S1. *C. crescentus* strains used in this study

Caulobacter strain	Relevant genetic markers/ description	Construction, source, or ref.
C. crescentus CB15N	Synchronizable derivative of *C. crescentus CB15*	1
MT190 (JP196)	CB15N *cfp-parB*	2
NR1751	CB15N Δ*tipN*	3
GB255	CB15N Δ*popZ*	4
JP308	CB15N P_{vanA}::*parA-eyfp (G16V)*	Single integration of pJP232 into CB15N
JP258	CB15N P_{vanA}::*parA-eyfp (G16V)*, Δ*tipN*	Single integration of pJP232 into NR1751
JP437	CB15N P_{vanA}::*parA-eyfp (G16V)*, Δ*popZ*	Single integration of pJP232 into GB255
JP443	CB15N P_{vanA}::*parA-eyfp (G16V)*, Δ*popZ*, pBXMCS4-tipN-mcherry	Single integration of pJP264 into JP437
JP88	CB15N *parA-m2*	pJP62 into CB15N (double homologous recombination)
GB308 (JP446)	CB15N *cfp-parB*, Δ*popZ*	4
JP468	CB15N *cfp-parB, mcherry-popZ*	Single integration of pJP289 into GB308
JP502	CB15N *cfp-parB, mcherry-popZ (E12K/R19E)*	Single integration of pJP387 into GB308
JP470	CB15N *cfp-parB, mcherry-popZ (S22P)*	Single integration of pJP312 into GB308
JP451	CB15N *cfp-parB, mcherry-popZ (E12K/R19E/S22P)*	Single integration of pJP347 into GB308
GB902	CB15N *cfp-parB,* Δ*popZ*, P_{xylX}-*parA-eyfp (G16V)*	Single integration of pJP45 into GB308
Strain 241	CB15N P_{vanA}::*parA-eyfp (G16V), cfp-parB,* Δ*popZ*, pBXMCS4-popZ	Transformation of plasmid 172 into GB902
Strain 242	CB15N P_{vanA}::*parA-eyfp (G16V), cfp-parB,* Δ*popZ*, pBXMCS4-*popZ (E12K/R19E)*	Transformation of pGB908 into GB902
Strain 255	CB15N P_{vanA}::*parA-eyfp (G16V), cfp-parB,* Δ*popZ*, pBXMCS4-popZ (S22P)	Transformation of plasmid 248 into GB902
JP461	CB15N P_{vanA}::*pamcherry-popZ*	Single integration of pJP413 into CB15N
JP464	CB15N P_{vanA}::*pamcherry-popZ*, P_{xylX}-*parA-eyfp (G16V)*	Single integration of pJP420 into JP461
JP465	CB15N P_{vanA}::*pamcherry-popZ*, P_{xylX}-*eyfp-parB*	Single integration of pJP384 into JP461

1. Evinger M, Agabian N (1977) Envelope-associated nucleoid from Caulobacter crescentus stalked and swarmer cells. *J Bacteriol* 132(1):294–301.
2. Thanbichler M, Shapiro L (2006) MipZ, a spatial regulator coordinating chromosome segregation with cell division in Caulobacter. *Cell* 126(1):147–162.
3. Huitema E, Pritchard S, Matteson D, Radhakrishnan SK, Viollier PH (2006) Bacterial birth scar proteins mark future flagellum assembly site. *Cell* 124(5):1025–1037.
4. Bowman GR, et al. (2008) A polymeric protein anchors the chromosomal origin/ParB complex at a bacterial cell pole. *Cell* 134(6):945–955.

Table S2. *E. coli* strains used in this study

E. coli strain	Plasmid(s) maintained	Genetic background
eJP472	pET28b-*parA-6His*	Rosetta(DE3) pLysS
eJP201	pET28b-*6His-parB*	Rosetta(DE3) pLysS
eJP446	pET28b-*6His-popZ*	BL21(DE3)
eJP593	pACYCduet1-*parA-eyfp (K20Q)*, pASKIBA3+*mcherry-popZ*	BL21(DE3)
eJP592	pACYCduet1-*parA-eyfp (G16V)*, pASKIBA3+*mcherry-popZ*	BL21(DE3)
eJP591	pACYCduet1-*parA-eyfp (R195E)*, pASKIBA3+*mcherry-popZ*	BL21(DE3)
eJP594	pACYCduet1-*parA-eyfp (D44A)*, pASKIBA3+*mcherry-popZ*	BL21(DE3)
eJP590	pACYCduet1-*parA-eyfp*, pASKIBA3+*mcherry-popZ*	BL21(DE3)
eJP595	pACYCduet1-*parA-eyfp (D44A/R195E)*, pASKIBA3+*mcherry-popZ*	BL21(DE3)
eJP290	pCDFduet1-*parB*, pACYCduet1-*parA-eyfp*	BL21(DE3)
eJP606	pASKIBA3+*mcherry-popZ*, pCDFduet1-*parB*, pACYCduet1-*parA-eyfp*	BL21(DE3)
eJP607	pASKIBA3+*mcherry-popZ (E12K/R19E*), pCDFduet1-*parB,* pACYCduet1-*parA-eyfp*	BL21(DE3)
eJP608	pASKIBA3+*mcherry-popZ (S22P)*, pCDFduet1-*parB* pACYCduet1-*parA-eyfp*	BL21(DE3)
eJP609	pASKIBA3+*mcherry-popZ*, pCDFduet1-*parB (L12A),* pACYCduet1-*parA-eyfp*	BL21(DE3)
eJP610	pCDFduet1-*parB (L12A)*, pACYCduet1-*parA-eyfp*	BL21(DE3)
e118	pACYCduet1-*cfp-parB*, *parA-eyfp (G16V)*	BL21(DE3)
eJP619	pBad/HisA-*popZ*, pACYCduet1-*cfp-parB-parAeyfp (G16V)*	BL21(DE3)
eJP620	pBad/HisA-*popZ (E12K/R19E)*, pACYCduet1-*cfp-parB-parAeyfp (G16V)*	BL21(DE3)
eJP621	pBad/HisA-*popZ (E12K/R19E/S22P)*, pACYCduet1-*cfp-parB-parAeyfp (G16V)*	BL21(DE3)
eJP622	pBad/HisA-*popZ (S22P)*, pACYCduet1-*cfp-parB-parAeyfp (G16V)*	BL21(DE3)

Table S3. Plasmids used in this study

Plasmid	Description	Source or ref.
pXYFPC-2	Integration of C-terminal eyfp-fusions at *Caulobacter* p-xylx locus (kanr)	1
pXYFPN-4	Integration of N-terminal eyfp-fusions at *Caulobacter* p-xylx locus (gentr)	1
pBXMCS-4	High-copy plasmid for xylose-inducible expression in *Caulobacter* (gentr)	1
pVYFPC-5	Integration of C-terminal eyfp-fusions at *Caulobacter* p-vana locus (tetr)	1
pXYFPN-2	Integration of N-terminal eyfp-fusions at *Caulobacter* p-xylx locus (kanr)	1
pMCS-4	Vector for chromosomal integration in *Caulobacter* (gentr)	1
pNPTS138	Gene replacement in *Caulobacter* by homologous recombination (kanr)	M. Alley, unpublished
pCDFduet1	*E. coli* expression vector with tandem T7 promoters	Novagen
pET28b	*E. coli* expression vector with T7 promoter	Novagen
pASKIBA3+	*E. coli* expression vector with Tet promoter	Neuromics
pACYCduet1	*E. coli* expression vector with tandem T7 promoters	Novagen
pBad/HisA	*E. coli* expression vector with pAra promoter	Invitrogen
pJP232	pVYFPC5-*parA-eyfp (G16V)*	This study
pJP264	pBXMCS4-*tipN-mcherry*	This study
pJP62	pNPTS138 *parA-M2*	This study
pJP325	pET28b-*parA-6His*	This study
pGB165	pET28b-*6His-parB*	This study
pGB165	pET28b-*6His-popZ*	2
pJP382	pET28b-*6His-popZ (S22P)*	This study
pJP383	pET28b-*6His-popZ (E12K/R19E)*	This study
pJP408	pET28b-*6His-popZ (E12K/R19E/S22P)*	This study
pGB759	pASKIBA3+*mcherry-popZ*	This study
pJP410	pASKIBA3+*mcherry-popZ (E12K/R19E)*	This study
pJP411	pASKIBA3+*mcherry-popZ (S22P)*	This study
pJP94	pACYCduet1-*parA-eyfp (G16V)*	3
pJP95	pACYCduet1-*parA-eyfp (K20Q)*	3
pJP89	pACYCduet1-*parA-eyfp (R195E)*	3
pJP96	pACYCduet1-*parA-eyfp (D44A)*	3
pJP88	pACYCduet1-*parA-eyfp*	3
pJP305	pACYCduet1-*parA-eyfp (D44A/R195E)*	3
pJP186	pCDFduet1-*parB*	This study
Plasmid 118	pACYCduet1-*parA-eyfp (G16V)-cfp-parB*	This study
pJP414	pBad/HisA-*popZ*	This study
pJP415	pBad/HisA-*popZ (E12K/R19E)*	This study
pJP417	pBad/HisA-*popZ (E12K/R19E/S22P)*	This study
pJP318	pBad/HisA-*popZ (S22P)*	This study
pJP289	pMCS4-P*popZ-mcherry-popZ*	This study
pJP387	pMCS4-P*popZ-mcherry-popZ (E12K/R19E)*	This study
pJP312	pMCS4-P*popZ-mcherry-popZ (S22P)*	This study
pJP347	pMCS4-P*popZ-mcherry-popZ (E12K/R19E/S22P)*	This study
pJP403	pXYFPN4-*popZ*	This study
pJP413	pVPamcherryN5-*popZ*	This study
pJP420	pXYFPC2-*parA (G16V)*	This study
pJP45	pXYFPC5-*parA (G16V)*	3
Plasmid 248	pBXMCS4-*popZ (S22P)*	This study
pGB172	pBXMCS4-*popZ*	4
pGB908	pBXMCS4-*popZ (E12K/R19E)*	This study
pJP384	pXYFPN2-*parB*	This study

1. Thanbichler M, Iniesta AA, Shapiro L (2007) A comprehensive set of plasmids for vanillate- and xylose-inducible gene expression in Caulobacter crescentus. *Nucleic Acids Res* 35(20):e137.
2. Bowman GR, et al. (2008) A polymeric protein anchors the chromosomal origin/ParB complex at a bacterial cell pole. *Cell* 134(6):945–955.
3. Ptacin JL, et al. (2010) A spindle-like apparatus guides bacterial chromosome segregation. *Nat Cell Biol* 12(8):791–798.
4. Bowman GR, et al. (2010) Caulobacter PopZ forms a polar subdomain dictating sequential changes in pole composition and function. *Mol Microbiol* 76(1):173–189.